International Journal of Recent Innovations in Academic Research
E-ISSN: 2635-3040; P-ISSN: 2659-1561
Homepage: https://www.ijriar.com/
Volume-9, Issue-3, July-September-2025: 276-284

Research Article

Sustainable Biopolymer and Basalt-Derived Filters for Enhanced Water Purification

Justin Chun

Independent Researcher, Iolani School, USA
Email: justinchun07@gmail.com

Received: August 14, 2025 **Accepted:** September 02, 2025 **Published:** September 08, 2025

Abstract
This study aimed to develop environmentally friendly and sustainable water purification techniques by developing chitosan beads, alginate beads and PAA-modified basalt, and subsequently evaluating their removal performance against heavy metals (Co, Cd, Cu, Pb) and emerging contaminants (MC-LR and microplastics). Surface functional groups of the sorbents were characterized using FT-IR, while adsorption experiments were conducted to determine removal efficiencies and propose underlying mechanisms. The results demonstrated that chitosan beads effectively removed Cu^{2+} and MC-LR through electrostatic interactions and hydrogen bonding of amine groups. Alginate beads exhibited superior performance for Cd^{2+} and Pb^{2+} removal, attributed to ion-exchange reactions mediated by abundant carboxyl groups. PAA-modified basalt achieved the highest efficiency for Co^{2+} and microplastic removal, driven by its porous structure, high surface area, and introduced carboxyl functionalities. Overall, these findings highlight the critical role of interactions between the physiochemical properties of pollutants and the surface functionalities of sorbents and suggest that hybrid sorbent systems may provide an effective strategy for addressing complex, multi-pollutant water environments.
Keywords: Adsorption, Surface Modification, Biopolymer, Basalt, Emerging Pollutants.

1. Introduction

Water pollution is a serious problem that harms people's health and the balance of nature all over the world, and keeping water safe to use has become an important challenge for building a sustainable society. Even though current purification methods work well, they often cannot handle emerging pollutants (Teodosiu *et al.,* 2018). In addition, filters made from synthetic polymers or activated carbon are not eco-friendly enough, raising concerns about their long-term use (Kamath *et al.,* 2022).

Recent research shows that harmful pollutants such as heavy metals and toxins from cyanobacteria (like microcystin) are increasing due to climate change (Wood *et al.,* 2017), and microplastics from growing plastics use are not fully removed by today's purification systems. These pollutants often remain in treated water. They can cause slow but serious damage to human health or build up in the food chain, showing the urgent need for better purification methods.

Heavy metals are especially dangerous because they are very toxic and stay in the environment for a long time (Ali *et al.,* 2019), which is why strict regulations have been made by groups like World Health Organization (WHO) and the U.S. Environmental Protection Agency (USEPA). Microcystin-LR (MC-LR), a toxic chemical from harmful algal blooms, is another strong risk (Malta *et al.,* 2022).

The WHO says drinking water should be less than 1 μg/L of MC-LR (Ríos *et al.,* 2013). This toxin damages the liver and can also lead to other pollution problems. Microplastics is also a big issue. They are very small, hard to remove with normal filters, and can build up in living things, creating long-term risks (Hale *et al.,* 2020). Together, these problems show the need for new filter materials that can clean many pollutants using one filtration system.

In this study, three materials were developed: Surface modified basalt, chitosan beads and alginate beads. Basalt, a natural rock with many tiny holes, is effective for filtering using their pore, and its surface

modification enhanced the capability to capture specific pollutants. Next, chitosan, a natural biopolymer containing amine groups, binds strongly to heavy metals and offers biodegradability with environmental safety. Finally, alginate, obtained from seaweed, forms stable beads through ionic interaction with metal ions, providing both pollutant removal capacity and biological safety.

The removal performance of these materials was evaluated against various pollutants. Chitosan and alginate beads showed effectiveness in controlling heavy metals, whereas the improved basalt was applied to remove microcystin-LR and microplastics. The mechanism of pollutant removal was investigated, and the capability of the materials under artificial contaminated water conditions was assessed.

In summary, this research presents a potential solution to overcome the limitations of existing commercial water purification systems by developing environmentally friendly and practical filtration systems. Accordingly, the developed materials hold promise for application not only in large-scale water purification facilities but also in household filtration units and industrial water recycling facilities. These findings highlight the potential of the proposed materials to serve as a sustainable and effective strategy for controlling multiple pollutants and advancing future water management practices.

2. Methods

2.1. Materials

Low molecular weight chitosan for the preparation of chitosan beads was purchased from Sigma-Aldrich Korea. Glacial acetic acid and sodium hydroxide beads used for the preparation of chitosan solutions were obtained from Duksan Science (Korea). Sodium alginate and calcium chloride, employed for the fabrication of alginate beads, were supplied by Sigma-Aldrich, Korea. Polyacrylic acid (PAA), used for the surface modification of basalt, was obtained from Sigma-Aldrich, Korea.

Genipin, used as a cross-linking reagent following surface modification, was purchased from Junsei Chemical (Japan). For pollutant removal, standard heavy metal solutions were obtained from Sigma-Aldrich (Korea). Microcystin-LR (MC-LR) was supplied by Enzo Life Science (USA), and micro particles based on polystyrene used in microplastic removal tests were purchased from Sigma-Aldrich (Korea).

2.2. Preparation of Sorbents

Low molecular weight chitosan, sodium alginate, calcium chloride, acetic acid glacial, and sodium hydroxide were used for bead preparation. For chitosan beads, 30g of chitosan was dissolved in 1L of 5% (v/v) acetic acid under stirring, stored at 4°C for 12 hrs to remove bubbles, and then dropped into a 1 M sodium hydroxide solution to form beads. The beads were washed with distilled water at least three times and stored in distilled water. For alginate beads, 20g of sodium alginate was dissolved in 1L of distilled water, kept at 4°C for 12 hrs to remove bubbles, and subsequently dropped into a 2% (w/v) calcium chloride solution. The beads were rinsed three times with distilled water and stored in distilled water until use.

Basalt was pretreated by washing with distilled water under stirring (300 rpm, five cycles), followed by immersion in 10% hydrochloric acid to remove impurities. The acid-treated basalt was rinsed with distilled water at least five times and oven-dried. Surface modification was performed by immersing 15g of dried basalt in 1L of 2% (w/v) polyacrylic acid (PAA) solution under stirring at 150 rpm for 8 h. After washing with distilled water three times to remove unreacted PAA, the modified basalt was immersed in a 1g/L genipin solution and stirred at 150 rpm for 12 hrs to induce cross-linking. The final product was thoroughly washed (more than 5 times), frozen and freeze-dried for subsequent use.

2.3. Analysis of Surface Functional Groups of Sorbents

Fourier-transform infrared spectroscopy (FT-IR) was employed to analyze changes in surface functional groups of the prepared sorbents, including chitosan beads, alginate beads and basalt-based materials. FT-IR spectra were recorded using FT-IR spectrophotometer (Agilent Technologies, USA) in the range of 650-4,000 cm^{-1}. Samples analyzed included alginate beads, chitosan beads, pristine basalt, and polyacrylic acid (PAA)-modified basalt.

2.4. Adsorption Experiments

Batch adsorption experiments were conducted to evaluate the removal performance of the prepared sorbents (chitosan beads, alginate beads, and PAA-modified basalt) against four heavy metals and two emerging contaminants, namely microcystin-LR (MC-LR) and microplastics. For the heavy metal adsorption tests, standard solutions of Pb, Cd, Co, and Cu were prepared at an initial concentration of 100mg/L. Each

sorbent (0.5g) was added to the solutions, and adsorption performance was evaluated under identical conditions. The residual concentrations of the heavy metals were quantified using inductively coupled plasma-optical emission spectroscopy (ICP-OES). All experiments were performed in triplicate to ensure reproducibility.

For MC-LR adsorption tests, a stock solution (2,000mg/L) was prepared by dissolving 2mg of MC-LR standard in 2mL of methanol. The stock solution was subsequently diluted with deionized water to obtain the desired concentration. Each sorbent (0.5g) was suspended in 25mL of MC-LR solution (200ug/L) and agitated at 150 rpm using a shaker. Aliquots were collected at predetermined time intervals and the residual MC-LR concentration was determined to calculate removal efficiency.

For the microplastic removal tests, artificial microplastic suspensions were prepared as model solutions. Each sorbent (0.5g/50mL) was introduced into the suspension and agitated at 150 rpm. At predetermined time interval, aliquots of the supernatant were collected and the residual microplastic particle size distribution was analyzed using dynamic light scattering (DLS) to assess removal efficiency.

2.5. Analysis of Heavy Metal and Emerging Contaminant Removal Efficiency

The removal efficiency of heavy metals (Pb, Cd, Co, and Cu) was evaluated using inductively coupled plasma-optical emission spectroscopy (ICP-OES, Agilent, USA). Prior to analysis, aqueous samples (1mL) were filtered through 0.2μm PTFE syringe filters to remove particulate matter and subsequently diluted tenfold with deionized water.

For the quantification of microcystin-LR (MC-LR), high-performance liquid chromatography equipped with a photodiode array detector (HPLC-PDA, Waters 515, USA) was employed. The mobile phase consisted of 42% acetonitrile containing 0.1% trifluoroacetic acid (TFA), filtered through a membrane to prevent clogging. The flow rate was maintained 0.1% trifluoroacetic acid (TFA), filtered through a membrane to prevent clogging. The flow rate was maintained at 1.5mL/min. Prior to injection, samples (1mL) were filtered through 0.2μm PTFE syringe filters. An injection volume of 200ul was loaded onto a YMC-Triart C18 column, and MC-LR was detected at 238nm. Quantitative analysis was performed using Empower 2 software (Waters, USA).

The removal efficiency of microplastics from artificially prepared suspensions was assessed by monitoring changes in particles size distribution of the supernatant using dynamic light scattering (DLS; Zetasizer, Malvern Panalytical, UK). All experiments were conducted in triplicate to ensure reproducibility.

3. Results and Discussion

3.1. Surface Functional Groups Properties of Developed Sorbents

To elucidate the removal mechanisms of the developed sorbents, Fourier-transform infrared spectroscopy (FT-IR) was first employed to analyze the surface functional groups of the three sorbents. Figure 1 presents the FT-IR spectrum of chitosan beads. The analysis revealed characteristic absorption bands at 3,400-3,200, 2,870, 1,650, 1,580, and 1,150 cm^{-1}. The broad band observed at 3,400-3,200 cm^{-1} corresponds to O-H and N-H stretching vibrations, indicative of an extensive hydrogen-bonding network (Sankararamakrishnan and Sanghi, 2006).

The peak at 2,870 cm^{-1} is associated with C-H stretching, representing alkyl group vibrations (Atangana *et al.,* 2019). In addition, the bands at 1,650 and 1,580 cm^{-1} can be assigned to the amide I (C=O stretching of residual acetyl groups) and N-H bending vibrations, respectively, confirming the presence of amine and residual acetamide functionalities (Kadir *et al.,* 2011).

Finally, the peak at 1,150 cm^{-1} corresponds to C-O-C and C-O stretching, characteristic of glycosidic linkages in the polysaccharide backbone (Pawlak and Mucha, 2003). Taking together, these results demonstrate that the chitosan beads possess abundant -OH and -NH_2 groups, glycosidic C-O-C linkages, and residual amide functionalities. These surface functional groups are expected to play a critical role in adsorption, particularly through hydrogen bonding, electrostatic interactions, and potential chelation with target contaminants.

Next, the surface functional groups of the developed alginate beads were further characterized by FT-IR spectroscopy (Figure 2). The spectrum revealed three major absorption bands at approximately 1,610, 1,410, and 1,080-1,020 cm^{-1}. The band at 1,610 cm^{-1} corresponds to the asymmetric stretching of carboxyl groups (-COO^-) (Sarmento *et al.,* 2006), whereas the band at 1,410 cm^{-1} is attributed to the symmetric stretching of -COO^- (Thombare *et al.,* 2023).

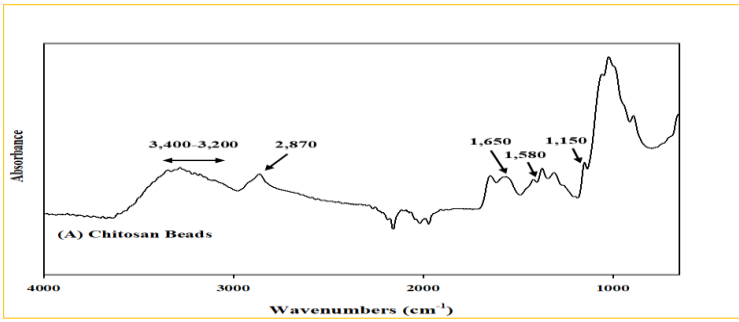

Figure 1. FT-IR spectrum of manufactured chitosan beads.

These two characteristic peaks together represent the distinctive doublet signature of alginate, commonly used as an indicator of metal ion crosslinking and ion-exchange processes within the polymer matrix. In addition, the absorption observed at 1,080-1,020 cm^{-1} is assigned to C-O-C glycosidic stretching, confirming the intact polysaccharide backbone of the alginate structure (Peniche-Pavía *et al.,* 2024). Collectively, the presence of the strong carboxylate doublet and glycosidic vibrations confirms that the prepared alginate beads retain the fundamental functional groups of alginates. Importantly, the dominance of carboxylate groups indicates that the surface charge of the beads is predominantly negative, governed by these functional moieties. This feature is critical in determining their adsorption behavior, as it directly influences electrostatic interactions with positively charged species and provides a mechanistic basis for ion-exchange during metal ion binding.

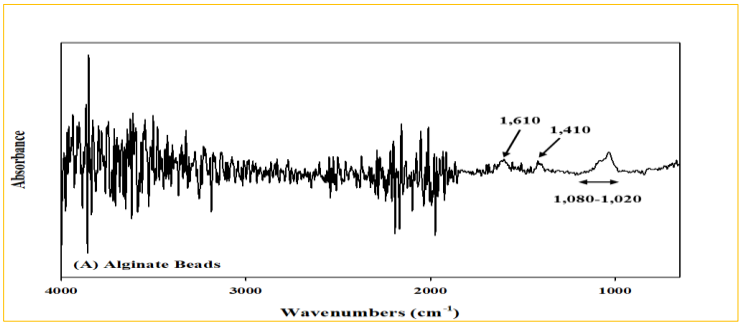

Figure 2. FT-IR spectrum of manufactured alginate beads.

Finally, the surface properties of the PAA-modified basalt were further investigated using FT-IR spectroscopy (Figure 3). The FT-IR spectrum revealed distinct peaks at 1,715-1,725, 1,550-1,590 and 1,100 cm^{-1}. The band observed at 1,715-1,725 cm^{-1} corresponds to the C=O stretching vibration of carboxylic acid groups (-COOH) (Thiruvasagam and Vijayan, 2012), providing direct evidence for the successful incorporation of PAA onto the surface of basalt. In addition, the peak at 1,550-1,590 cm^{-1} is attributed to the asymmetric stretching of carboxylate groups ($-COO^-$) (Pruneanu *et al.,* 1997), indicating partial ionization of PAA. This suggests that the introduced carboxylate functionalities can coordinate with surface metal cations of basalt or engage in strong electrostatic interactions. The prominent band at 1,100 cm^{-1} corresponds to the asymmetric stretching vibration of Si-O-Si bonds (Arigane *et al.,* 1999), characteristic of the aluminosilicate framework of basalt. The persistence of this signal confirms that the fundamental silicate backbone of basalt remained intact after surface modification. Collectively, these findings confirm the successful grafting of PAA onto basalt, while maintaining the structural integrity of the original mineral matrix.

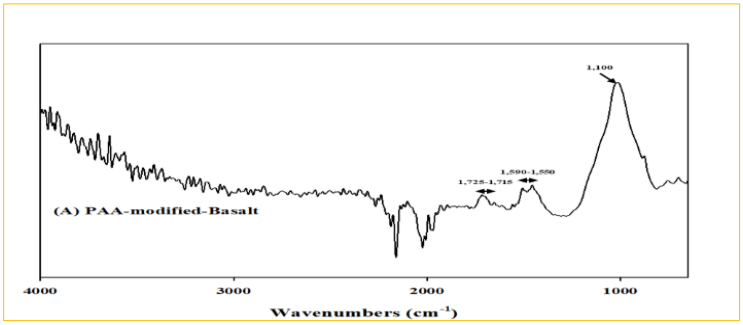

Figure 3. FT-IR spectrum of manufactured PAA-modified basalt.

From a mechanistic perspective, the presence of abundant carboxyl functional groups on the modified basalt surface enables strong electrostatic attraction and potential coordination with cationic heavy metal ions. In addition, the inherent high surface area and porous structure of basalt provide multiple active sites for physical adsorption and entrapment. Therefore, the PAA-modified basalt is expected to remove contaminants through a synergistic mechanism involving both chemical interactions (electrostatic and coordination bonding) and physical adsorption.

Taken together with the FT-IR analysis of chitosan beads, alginate beads and PAA-modified basalt, these results provide critical insight into the functional group composition of the three developed sorbents. Subsequent evaluations against target pollutants further elucidated how this surface functionalities govern the adsorption mechanism and removal efficiencies under environmentally relevant conditions.

3.2. Performance Comparison of Alginate Beads, Chitosan Beads, and PAA-Modified Basalt in Heavy Metal Removal

To evaluate the heavy metal removal potential of the three developed sorbents (PAA-modified basalt, alginate beads, and chitosan beads), four representative heavy metals (Co, Cd, Cu, and Pb) were selected. These metals were chosen because they are widely used in modern industrial processes while simultaneously contributing to environmental contamination. For cobalt removal, concentration changes were monitored at 5, 10, 30, and 60 min. Among the sorbents, PAA-modified basalt exhibited the highest removal efficiency, reaching 49.08±4.42 mg/L after 60 min. In contrast, chitosan beads demonstrated the lowest performance, with a removal efficiency of 28.70±0.59 mg/L at the same time point.

For cadmium removal, similar time intervals were applied. Alginate beads showed the highest performance, removing up to 63.27±1.51 mg/L within 60 min. As observed in cobalt removal, chitosan beads again exhibited the lowest efficiency, with only 26.06±0.97 mg/L removed. In the case of copper, a different trend was observed. Chitosan beads achieved the best performance, with a removal efficiency of 56.67±1.29 mg/L after 60 min. Conversely, alginate beads exhibited the lowest efficiency, with only 22.50±0.12 mg/L removed during the same period.

For lead removal, efficiency followed the order of PAA-modified basalt > alginate beads > chitosan beads. After 60 min, PAA-modified basalt achieved the highest removal (76.89±3.08 mg/L), followed by alginate beads (70.08±3.30 mg/L), while chitosan beads showed significantly lower performance (23.82±1.58 mg/L). These results highlight distinct differences in removal efficiencies depending on both the metal ion and the sorbent. To better understand these variations, mechanistic analyses were further conducted to correlate the adsorption performance with the physiochemical properties of the target metal ions, and the functional groups present on each sorbent surface.

The adsorptive removal performance of the three developed sorbents (alginate beads, chitosan beads, and PAA-modified basalt) toward Pb^{2+}, Cd^{2+}, Co^{2+}, and Cu^{2+} showed distinct differences depending on the physicochemical properties of the metal ions and the surface functionalities of the sorbents.

As shown in Figure 4A, PAA-modified basalt exhibited the highest removal efficiency for CO^{2+}. This result can be attributed to the introduction of carboxyl groups (-COOH) by PAA modification, which facilitated strong electrostatic attraction and surface complexation with Co^{2+} ion. In contrast, chitosan beads and alginate beads displayed relatively lower efficiencies. This may be explained by the high stabilization energy of Co^{2+}, which limits its ability to form stable complexes with amine ($-NH_2$) or carboxyl (-COOH) groups. For Cd^{2+} removal (Figure 4B), alginate beads demonstrated significantly higher adsorption capacity compared with the other sorbents. Superior performance can be ascribed to the abundance of carboxyl groups in alginate, which enhance ion exchanges and complexation with Cd^{2+}.

Moreover, the relatively large ionic radius of Cd^{2+} allows for stable binding within the alginate gel network, where multiple coordination sites are available. PAA-modified basalt and chitosan beads showed moderate removal efficiency, which is likely due to the weaker binding affinity of Cd^{2+} compared to Pb^{2+} or Cu^{2+}, thereby limiting interactions with amine or carboxyl functionalities. In the case of Cu^{2+} removal (Figure 4C), chitosan beads achieved the highest adsorption efficiency. This can be explained by the strong chelation ability of amine groups in chitosan, which readily form stable complexes with Cu^{2+}. The high affinity promotes strong coordination with nitrogen ligands. Consequently, chitosan-based sorbents exhibited superior performance toward Cu^{2+} compared to the other sorbents. In contrast, alginate beads showed relatively low affinity for Cu^{2+}, whereas PAA-modified basalt demonstrated intermediate performance.

As shown in Figure 4D, the removal of Pb^{2+} was significantly higher for alginate beads and chitosan beads compared to PAA-modified basalt. This can be attributed to the relatively large ionic radius of Pb^{2+}, which allows for the formation of stable complexes with oxygen- and nitrogen-containing ligands. In particular, the carboxyl groups of alginates and the amine groups of chitosan provide strong coordination sites, resulting in rapid and highly efficient Pb^{2+} removal. In contrast, despite the increased negatively charge density introduced through surface modification, PAA-modified basalt exhibited comparatively lower performance. This result suggests that the rapid diffusion and binding characteristics of Pb^{2+} were not fully accommodated by the modified basalt surface.

Taken together, these findings indicate that heavy metal removal performance is governed by the interplay of various factors of heavy metal and sorbents. Cu^{2+} exhibited strong affinity for nitrogen ligands, leading to superior removal efficiency in chitosan. Pb^{2+}, by contrast, formed stable complexes with both oxygen- and nitrogen-containing ligands, which resulted in high removal efficiencies by alginate and chitosan beads. Cd^{2+} showed strong removal performance in alginate due to ion exchanges interactions, while Co^{2+} removal was most effective with PAA-modified basalt, likely driven by strong electrostatic interactions with the negatively charged surface. Overall, the results highlight the clear correlation between sorbent functionalities and the physicochemical properties of target metal ions, providing valuable insights into the design of selective sorbents for multi-contaminant environments. Furthermore, the complementary performance of the different sorbents suggests that composite or sequential applications could be strategically employed to enhance treatment efficiency under complex heavy metal contamination scenarios.

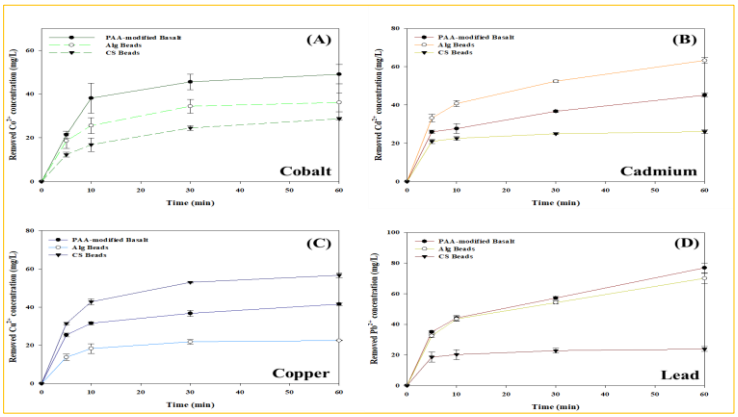

Figure 4. Removal efficiencies of PAA-modified basalt, alginate beads, and chitosan beads toward four heavy metals: (A) cobalt, (B) cadmium, (C) copper, and (D) lead.

3.3. Performance Comparison of Alginate Beads, Chitosan Beads, and PAA-Modified Basalt in Emerging Contaminants Removal

To examine whether the three developed sorbents could be extended beyond heavy metal purification to the control of emerging pollutants, their performance was evaluated against microcystin-LR (MC-LR), a cyanobacterial toxin frequently associated with harmful algal blooms, and polystyrene microplastics.

For MC-LR removal, a 200 ppb aqueous solution was treated with each sorbent, and residual concentrations were monitored at 30, 60, 120, 240, 480, 720, 1440, and 2880 min. As shown in Figure 5, chitosan (CS) beads exhibited the highest removal efficiency, achieving the removal of 164.70±2.10 ppb of MC-LR after 48 h. PAA-modified basalt also demonstrated considerable removal, with 153.25±1.50 ppb removed within the same period. In contrast, alginate beads exhibited negligible removal capacity, achieving only 69.46±1.47 ppb reduction after 48 h. These results indicate that the three sorbents follow distinct removal mechanisms governed by their physicochemical surface properties.

The superior performance of chitosan beads can be attributed to their abundance of amine and hydroxyl groups. Under slightly acidic to neutral conditions, amine groups are protonated ($-NH_3^+$), enabling strong electrostatic interactions with the negatively charged functional groups of MC-LR, such as carboxylate and methoxy groups. In addition, hydrogen bonding and potential chelation between amine groups and the peptide backbone or polar regions surrounding the Adda moiety further enhanced sorption, leading to high removal efficiency. In the case of PAA-modified basalt, the porous structure and large surface are if the basalt contributed to its adsorption performance. However, its removal efficiency was lower than that of chitosan beads. This is likely due to the carboxyl groups (-COOH) introduced by PAA modification, which imparted on

overall negative surface charge. As a result, electrostatic repulsion occurred between the sorbent surface and the negatively charged MC-LR molecules in aqueous solution, limiting sorption capacity despite the favorable surface area. By contrast, alginate beads exhibited poor removal efficiency. Although alginate contains abundant carboxyl groups, which are advantageous for binding cationic heavy metals, they are ineffective for neutral or anionic organic toxins such as MC-LR. The negatively charged alginate surface induced electrostatic repulsion with MC-LR, thereby reducing adsorption efficiency. This suggests that alginate-based sorbents are not suitable for MC-LR removal although their performance could potentially be improved through surface modification or the introduction of additional functional groups.

Taken together, these findings demonstrate that chitosan beads are the most effective material for controlling MC-LR among the three sorbents, primarily due to the role of amine groups in electrostatic interactions and hydrogen bonding. PAA-modified basalt exhibited moderate removal efficiency, driven by its porous structure and surface functionalities, while alginate beads showed significant structural and electrostatic limitations. These results highlight the importance of understanding the interplay between surface of sorbent and target pollutant properties when designing effective sorbents. Moreover, they suggest that combining sorbent with complementary properties may offer a promising platform for the remediation of diverse contaminants, including both heavy metals and emerging organic pollutants.

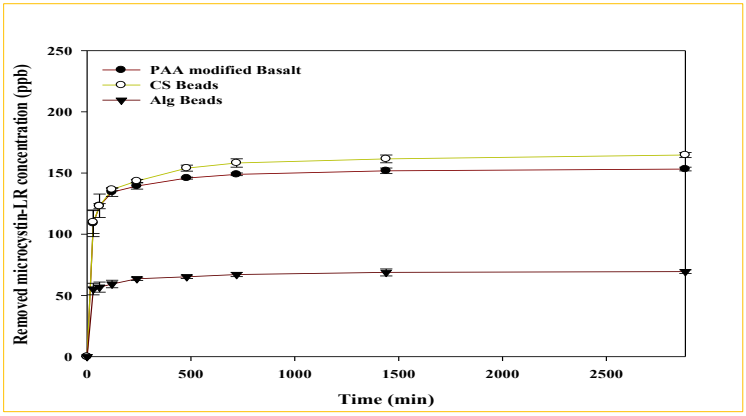

Figure 5. Comparative assessment of MC-LR removal efficiency over 48 h using chitosan beads, alginate beads and PAA-modified basalt.

In addition to microcystin removal, the removal efficiency of emerging contaminants, specifically microplastics (which have recently attracted significant concern due to their environmental and health impacts), was evaluated using the three developed sorbents. The average particle size of the supernatant was monitored over a 48 h following treatment (Figure 6). In the control group, the particle size remained stable within the range of 1.8-2.0μm, indicating that no substantial removal or degradation of microplastics occurred in the absence of sorbent treatment.

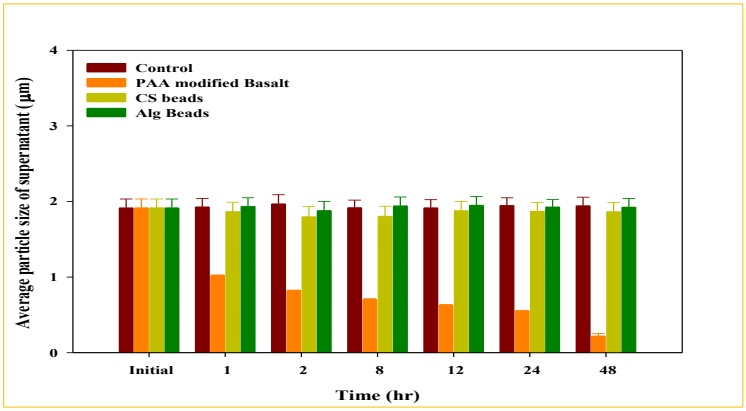

Figure 6. Comparative analysis of supernatant particle size reduction in control and sorbent treated systems containing polystyrene microplastics.

In contrast, treatment with PAA-modified basalt resulted in a progressive decrease in the average particle size of the supernatant, reaching values below 0.5μm after 48 h. These results suggest that the negatively

charged surface of PAA-modified basalt established strong electrostatic interactions with microplastic particles, promoting surface-mediated aggregation and facilitating their removal from suspension. Furthermore, basalt inherently possesses a highly porous structure and large specific surface area, which provides numerous active sites for the physical adsorption and entrapment of microplastics. These intrinsic structural features, in synergy with the introduced carboxyl functional groups from PAA modification, appear to enhance both electrostatic interactions and physical trapping, thereby supporting a dual mechanism of removal.

In contrast, both chitosan beads and alginate beads exhibited negligible changes in supernatant particle size over 48 h, showing trends similar to the control. This limited performance can be attributed to differences in surface properties. Chitosan beads, while rich in amine groups that are positively charged under slightly acidic to neutral conditions, are more effective in removing negatively charged contaminants such as cyanotoxins but exhibit limited affinity toward hydrophobic polystyrene microplastics. Alginate beads, on the other hand, contain abundant carboxyl groups that confer a negative surface charge. Consequently, electrostatic repulsion between the surface of alginate and negatively charged polystyrene microplastics likely suppressed adsorption efficiency, resulting in minimal removal.

Overall, these findings demonstrate that PAA-modified basalt was the most effective sorbent for microplastic removal, owing to the combined contributions of its porous structure, large surface area, electrostatic attraction, hydrophobic interactions, and surface-mediated aggregation. In contrast, chitosan-and alginate-based beads were not effective for microplastic removal. Importantly, this outcome highlights that in complex pollution scenarios, where multiple classes of contaminants coexist, composite materials incorporating complementary functional groups may provide a more versatile and robust platform for water purification applications.

4. Conclusions

In this study, three environmentally sustainable sorbents (chitosan beads, alginate beads and PAA-modified basalt) were developed and their removal performances against heavy metals and emerging pollutants were systemically evaluated. The results demonstrated that chitosan beads were most effective in removing copper ions and the cyanobacterial toxin microcystin-LR, primarily through electrostatic interactions and hydrogen bonding mediated by amine groups. Alginate beads exhibited superior performance in cadmium and lead removal due to ion exchanges facilitated by abundant carboxyl groups. In contrast, PAA-modified basalt achieved the highest efficiency in cobalt and microplastic removal, attributed to the combined effects of its porous structure, large surface area, and carboxyl functionalities introduced via surface modification.

These findings highlight that removal efficiency is largely governed by the interplay between sorbent surface functionalities and the physiochemical properties of the target pollutants. Importantly, they suggest that under real conditions, where multiple classes of pollutants coexist, the application of composite or sequential sorbent platform with complementary properties may represent a more effective and sustainable strategy for advanced water purification.

Declarations

Acknowledgements: The author thank the laboratory for the support during the research.
Author Contribution: The author confirms sole responsibility for the following: study conception and design, data collection, analysis and interpretation of results, and manuscript preparation.
Conflict of Interest: The author declares no conflict of interest.
Consent to Publish: The author agrees to publish the paper in International Journal of Recent Innovations in Academic Research.
Data Availability Statement: The data presented in this study are available upon request from the author.
Funding: This research received no external funding.
Institutional Review Board Statement: Not applicable.
Informed Consent Statement: Not applicable.
Research Content: The research content of the manuscript is original and has not been published elsewhere.

References

1. Ali, H., Khan, E. and Ilahi, I. 2019. Environmental chemistry and ecotoxicology of hazardous heavy metals: Environmental persistence, toxicity, and bioaccumulation. Journal of Chemistry, 2019(1): 6730305.

2. Arigane, T., Yoshida, K., Wadayama, T. and Hatta, A. 1999. In situ FT-IR and photoluminescence study of porous silicon during exposure to F2, H2O, and D2O. Surface Science, 427: 304-308.

3. Atangana, E., Chiweshe, T.T. and Roberts, H. 2019. Modification of novel chitosan-starch cross-linked derivatives polymers: Synthesis and characterization. Journal of Polymers and the Environment, 27(5): 979-995.

4. Hale, R.C., Seeley, M.E., La Guardia, M.J., Mai, L. and Zeng, E.Y. 2020. A global perspective on microplastics. Journal of Geophysical Research: Oceans, 125(1): e2018JC014719.

5. Kadir, M., Aspanut, Z., Majid, S.R. and Arof, A.K. 2011. FTIR studies of plasticized poly (vinyl alcohol)–chitosan blend doped with NH_4NO_3 polymer electrolyte membrane. Spectrochimica Acta Part A: Molecular and Biomolecular Spectroscopy, 78(3): 1068-1074.

6. Kamath, S.V., Mruthunjayappa, M.H., Mondal, D. and Kotrappanavar, N.S. 2022. Nanocomposite-based high-performance adsorptive water filters: Recent advances, limitations, nanotoxicity and environmental implications. Environmental Science: Nano, 9(7): 2320-2341.

7. Malta, J.F., Nardocci, A.C., Razzolini, M.T.P., Diniz, V. and Cunha, D.G.F. 2022. Exposure to microcystin-LR in tropical reservoirs for water supply poses high risks for children and adults. Environmental Monitoring and Assessment, 194(4): 253.

8. Pawlak, A. and Mucha, M. 2003. Thermogravimetric and FTIR studies of chitosan blends. Thermochimica Acta, 396(1-2): 153-166.

9. Peniche-Pavía, H.A., Tzuc-Naveda, J.D., Rosado-Espinosa, L.A. and Collí-Dulá, R.C. 2024. FTIR-ATR chemometric analysis on pelagic *Sargassum* reveals chemical composition changes induced by cold sample transportation and sunlight radiation. Journal of Applied Phycology, 36(3): 1391-1405.

10. Pruneanu, S., Resel, R., Leising, G., Brie, M., Graupner, W. and Oniciu, L. 1997. Structural investigations on polypyrrole and poly (vinyl chloride)–polypyrrole composite films. Materials Chemistry and Physics, 48(3): 240-245.

11. Ríos, V., Moreno, I., Prieto, A.I., Puerto, M., Gutiérrez-Praena, D., Soria-Díaz, M.E. and Cameán, A.M. 2013. Analysis of MC-LR and MC-RR in tissue from freshwater fish (*Tinca tinca*) and crayfish (*Procambarus clarkii*) in tench ponds (Cáceres, Spain) by liquid chromatography–mass spectrometry (LC–MS). Food and Chemical Toxicology, 57: 170-178.

12. Sankararamakrishnan, N. and Sanghi, R. 2006. Preparation and characterization of a novel xanthated chitosan. Carbohydrate Polymers, 66(2): 160-167.

13. Sarmento, B., Ferreira, D., Veiga, F. and Ribeiro, A. 2006. Characterization of insulin-loaded alginate nanoparticles produced by ionotropic pre-gelation through DSC and FTIR studies. Carbohydrate Polymers, 66(1): 1-7.

14. Teodosiu, C., Gilca, A.F., Barjoveanu, G. and Fiore, S. 2018. Emerging pollutants removal through advanced drinking water treatment: A review on processes and environmental performances assessment. Journal of Cleaner Production, 197: 1210-1221.

15. Thiruvasagam, P. and Vijayan, M. 2012. Synthesis of new diacid monomers and poly (amide-imide) s: Study of structure–property relationship and applications. Journal of Polymer Research, 19(3): 9845.

16. Thombare, N., Mahto, A., Singh, D., Chowdhury, A.R. and Ansari, M.F. 2023. Comparative FTIR characterization of various natural gums: A criterion for their identification. Journal of Polymers and the Environment, 31(8): 3372-3380.

17. Wood, S.A., Borges, H., Puddick, J., Biessy, L., Atalah, J., Hawes, I., Dietrich, D.R. and Hamilton, D.P. 2017. Contrasting cyanobacterial communities and microcystin concentrations in summers with extreme weather events: Insights into potential effects of climate change. Hydrobiologia, 785(1): 71-89.

Citation: Justin Chun. 2025. Sustainable Biopolymer and Basalt-Derived Filters for Enhanced Water Purification. International Journal of Recent Innovations in Academic Research, 9(3): 276-284.